Cortical sulci detection and tracking

Christophe Renault, Michel Desvignes, Marinette Revenu

CORTICAL SULCI DETECTION AND TRACKING

Christophe Renault, Michel Desvignes, Marinette Revenu

GREYC - ISMRA, 6, Boulevard Maréchal Juin,
14050 CAEN Cedex, FRANCE
Tel: (+33) 231 452 922
e-mail: christophe.renault@greyc.ismra.fr

ABSTRACT

Automatic labelling and identification of cerebral structure, like cortical sulci, are useful in neurology, surgery planning, etc… We propose a cortical sulci valley detection. The aim of the method is to achieve the sulci medial surface. The method applied on MRI data, is based on geometrical features (curvature) which doesn't require the accurate segmentation of the cerebral cortex. We use a sub-voxel precision tracking. The minimum curvature vector in each point allows successive displacement along the valley of sulci. Partial derivatives provide the differential characteristics.

1. INTRODUCTION

Human cortical sulci identification on 3D image is used in neurology, surgical planning, human brain mapping… Cortical sulci are landmarks and represent gross morphology to localise anatomical structures and functional areas with respect to these landmarks. Sulci are deep cortical folds and previous works are the automatic labelling of the superficial trace of the sulci on the surface of the brain [3]. This paper presents a method to detect the deep cortical fold without an accurate segmentation of brain tissue (white matter, grey matter, cerebro-spinal fluid), using curvature features. In fig. 1 an interactive drawing of the medial surface of sulci is superimposed with the MRI slice. Unlike works which start from the outer edge of sulcus to go toward the valley, we want to propagate the valley toward the outer edge, in the opposite path [6]. Then, the valley detection of sulcus is an important stage of the process. This valley detection is obtained by 3 dimensions curve tracking.

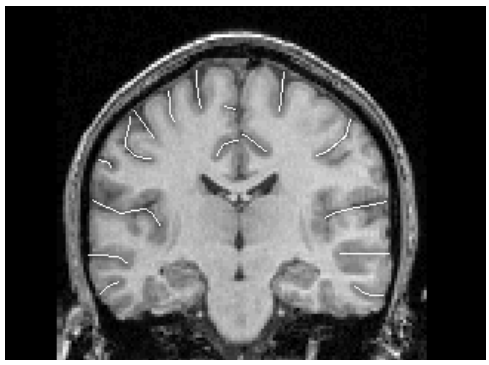

Figure 1: Medial surface of sulci superimposed with the MRI slice.

2. SULCI AND CURVATURE

Cortical sulci and gyri define gross anatomical landmarks on the surface of the cerebral cortex. Sulci represent the cortical folds. The parts between these convolutions are the gyri. Physical limits between sulci and gyri are not precisely defined, but respectively square with concave and convex parts. Curvature is then used to separate sulci and gyri. In 3D images, at each point A of an iso-surface *I*, there is an infinite number of directions in tangent plane of *I*. There are two principal directions $\vec{t}_1$ and $\vec{t}_2$, which correspond to the maximal and minimal curvature k_1 and k_2 (fig. 2) [4].

We define *K* and *S* the gaussian and average curvature:

$$K = k_1 k_2$$

$$S = \frac{k_1 + k_2}{2}$$

From differential characteristics of the image we compute *K* and S as following:

$$K = \frac{1}{h^2}\begin{pmatrix} I_x^2\left(I_{yy}I_{zz} - I_{yz}^2\right) + 2I_yI_z\left(I_{xz}I_{xy} - I_{xx}I_{yz}\right) + \\ I_y^2\left(I_{zz}I_{yy} - I_{xz}^2\right) + 2I_zI_x\left(I_{xy}I_{yz} - I_{yy}I_{xz}\right) + \\ I_y^2\left(I_{xx}I_{zz} - I_{xy}^2\right) + 2I_xI_y\left(I_{yz}I_{xz} - I_{zz}I_{xy}\right) \end{pmatrix}$$

$$S = \frac{1}{2h^{3/2}}\begin{pmatrix} I_x^2\left(I_{yy} + I_{zz}\right) - 2I_yI_zI_{yz} + \\ I_y^2\left(I_{zz} + I_{xx}\right) - 2I_zI_xI_{xz} + \\ I_z^2\left(I_{xx} + I_{yy}\right) - 2I_xI_yI_{xy} \end{pmatrix}$$

where $h = I_x^2 + I_y^2 + I_z^2$ and $I_{a^nb^m} = \frac{\partial^{n+m} I}{\partial a^n \partial b^m}$.

k_1 and k_2 are then obtained by:

$$k_{1,2} = S \pm \sqrt{S^2 - K}$$

and directions $\vec{t}_1$ and $\vec{t}_2$ by:

$$\overrightarrow{t_{1,2}} = \vec{\alpha} \pm \sqrt{S^2 - K}\,\vec{\beta}$$

with $\vec{\beta} = \left(I_z - I_y, I_x - I_z, I_y - I_x\right)$ and

$$\vec{\alpha}.\vec{x} = -\frac{1}{2h^{3/2}}\begin{pmatrix} -2I_z^3I_{xy} + I_y^3I_{zz} + 2I_y^3I_{xz} - 2I_y^2I_zI_{xy} \\ +2I_z^2I_xI_{yz} + 2I_z^2I_yI_{xz} - 2I_y^2I_xI_{yz} \\ -2I_xI_yI_zI_{zz} + 2I_xI_yI_zI_{yy} + I_y^2I_zI_{xx} \\ -2I_z^2I_xI_{xz} + I_x^2I_zI_{zz} - I_x^2I_zI_{yy} + 2I_z^2I_yI_{yz} \\ -I_y^2I_zI_{zz} + I_z^3I_{xx} - I_z^3I_{yy} - 2I_y^2I_xI_{xz} \\ +2I_x^2I_yI_{yz} - I_y^3I_{xx} + 2I_z^2I_xI_{xy} - I_z^2I_yI_{xx} \\ -2I_y^2I_zI_{yz} + I_z^2I_yI_{yy} - 2I_x^2I_zI_{yz} \\ +2I_y^2I_xI_{xy} + I_x^2I_yI_{zz} - I_x^2I_yI_{yy} \end{pmatrix}$$

The *y* an *z* components are obtained by circular permutations of *x*,*y* and *z*.

In case of sulci, $\vec{t}_2$ is along the valley. $\vec{t}_2$ will be used to follow the roof of sulci.

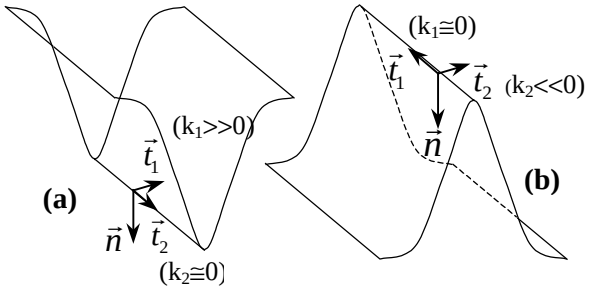

Figure 2: (a) Principal curvature on sulci, (b) Principal curvature on gyri.

3. 3D CURVE TRACKING

Sulci have to be represented as a parametric 3D curve, i.e. an ordered set of connected voxels (x(t),y(t),z(t)). The basic idea of the tracking process is to use the $\vec{t}_2$ vector, which give the direction of the next voxel for each point of the surface.

To achieve an iterative crest line tracking, we need three notions:

- Starting points, origin of 3D curve.
- A function which determines the next point of the curve, in local neighbourhood.
- A condition to stop the iterative process.

3.1. Discrete case

In the 3D discrete grid of the image we have noticed two main problems.

- In the direction of $\vec{t}_2$, we have to choice a voxel *V*. Now, there is only a finite number (26) of directions defined by the local neighbourhood.

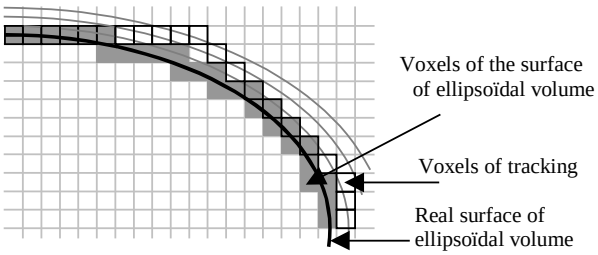

Figure 3: Discrete tracking

The tracking only moves in horizontal, vertical and diagonal directions (Fig.4) because of this restrictive choice of next voxels.

- Local curvature values are different from real values.

These two points lead the tracking process to fail to detect and to extract the sulci.

3.2. Subvoxel tracking

Since discrete derivative value are not accurate enough to ensure a precise detection, we used a sub-voxel tracking. Voxel notion is replaced by point notion, since the tracking goes step by step with a step smaller than voxel. The point positions are not in the grid of volume, so the differential characteristics are computed by trilinear or better interpolation.

Starting points

First, MLvv operator [1][2], similar to average curvature, is computed. Negative values of MLvv are kept by thresholding. The image is labelled and each connected component is a volume representing one sulcus. The starting points are the voxels with the highest curvature in each connected component.

Following points

Case 1:

From a point *P*, the next point *N* is the point in direction of the $\vec{t}_2$ vector, at the distance *step*. This method works in case of simple structures.

Exemple of ellipsoïdal structure:

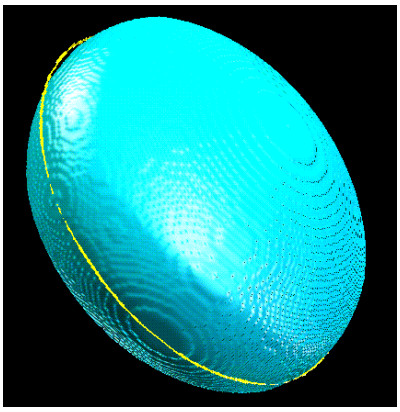

Figure 4: In white, the line corresponding to tracking on ellipsoïdal structure.

Case 2:

To deal with approximate value of curvature, the direction is a compromise between $\vec{t}_2$ and the direction of maximal curvature. A new direction $\vec{r}$ toward maximal average curvature is added to $\vec{t}_2$.

$$\vec{d} = \alpha \vec{t_2} + (1-\alpha)\vec{r}$$

where $$\vec{r} = \sum_{i=1}^{8} \frac{\overrightarrow{PM_i} C_i}{\|PM_i\|}$$

M_i are the 8 neighbour voxels of *P*, C_i their respective curvature. To avoid a tracking reverse, we impose the *case 3.*

Case 3:

$\vec{r}$ belong to the normal plan of $\vec{t}_2$ (Fig.5). The effect of $\vec{t}_2$ must be predominant

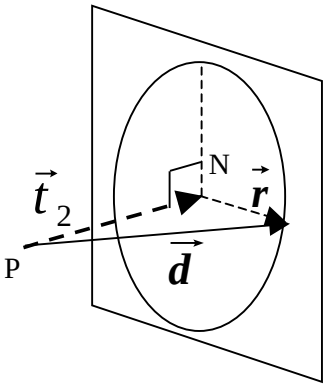

Figure 5: Direction $\vec{r}$ in normal plan of $\vec{t}_2$

Stopping conditions

This process is stopped when:

- The next voxel is in a gyri area (positive average curvature value).
- Umbilical area is reached: the principal curvatures K_1 and K_2 are equal, $\vec{t}_1$ and $\vec{t}_2$ are not defined in differential geometry.
- The curvatures are not defined: in area of nil gradient values.
- A junction with an other sulcus.

4. RESULTS

MRI of healthy volunteers were acquired on a 1.5 Tesla GE Signa scanner using a SPGR sequence (124*256*256 voxels, 1.3 mm3) (Fig. 6).

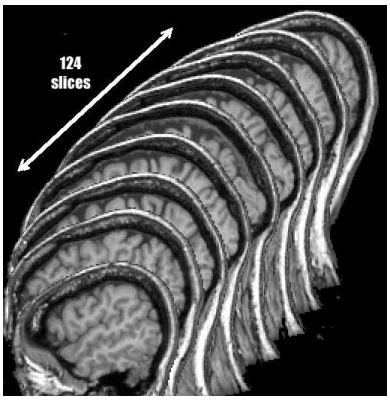

Figure 6: 124 MRI slices

Fig. 7 shows the result on a single sulcus. The white line is the result of the sub-voxel tracking (*case 3*). The grey part is a sulcus segmentation done by threshold of maximal curvature. On this Fig. 7. The tracking doesn't seem to be, in each point, on the roof of sulcus, because of viewpoints effect and non accurate segmentation of sulcus. However, replaced on the raw MRI slices, the tracking is visually located on the roof of sulcus.

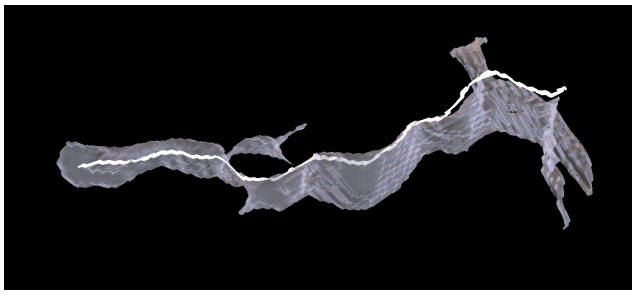

Figure 7: Result on a sulcus

5. Conclusion

We have presented a method to extract roof of sulci with a sub-voxel precision. This method uses MRI brain data without accurate segmentation of the cerebral cortex. Roof of sulci are represented as 3D parametric curve, these curves are easy to statistically handle (i.e. average curve, standard deviation) and are used to define an atlas of cerebral sulci.

References

[1] L. M. J. Florack, B. M. ter Haar Romeny, J. J. Koenderink, M. A. Viergever. "Scale and differential structure of images", *Image and Vision Computing*, Vol 10, July/August 1992, p 376-388.

[2] G. Le Goualher, C. Barillot, Y. Bizais, J-M Scarabin. "3D segmentation of cortical sulci using active models". *SPIE Proceedings of Medical Imaging*, Image Processing, 1996, volume 2710, p 254-263.

[3] N. Royackkers. "Modélisation et reconnaissance des Sillons du cortex cérébral humain". Ph.D Thesis, University of Caen, France, 1997.

[4] J.P. Thirion, A. Gourdon, "The Marching Lines Algorithm: new results and proofs". INRIA, Research report n° 1881, April 1993.

[5] G. Le Goualher, C. Barillot, Y. Bizais. "Modeling Cortical Sulci with Active Ribbons". *Int. J. of Pattern Recognition and Artificial Intelligence*, 1997, Vol 11(8), pp. 1295-1315.

[6] M. Vaillant, C. Davatzikos, R. N. Bryan, "Finding 3D Parametric Representations of the Deep Cortical Folds". Proc. of the IEEE Workshop on Mathematical Methods, *Biomedical Image Analysis*, June 1996, pp 151-159.